Journal of Molecular and Cellular Cardiology 117 (2018) 72–81

Contents lists available at ScienceDirect

Journal of Molecular and Cellular Cardiology

journal homepage: www.elsevier.com/locate/yjmcc

Original article

Hypertrophic cardiomyopathy mutation R58Q in the myosin regulatory light chain perturbs thick filament-based regulation in cardiac muscle

Thomas Kampourakis*, Saraswathi Ponnam, Malcolm Irving

Randall Centre for Cell and Molecular Biophysics, British Heart Foundation Centre of Research Excellence, King's College London, London SE1 1UL, United Kingdom

ARTICLE INFO

Keywords:
Myosin
Cardiac muscle regulation
Myosin regulatory light chain
Polarized fluorescence
Hypertrophic cardiomyopathy

ABSTRACT

Hypertrophic cardiomyopathy (HCM) is frequently linked to mutations in the protein components of the myosin-containing thick filaments leading to contractile dysfunction and ultimately heart failure. However, the molecular structure-function relationships that underlie these pathological effects remain largely obscure. Here we chose an example mutation (R58Q) in the myosin regulatory light chain (RLC) that is associated with a severe HCM phenotype and combined the results from a wide range of *in vitro* and *in situ* structural and functional studies on isolated protein components, myofibrils and ventricular trabeculae to create an extensive map of structure-function relationships. The results can be understood in terms of a unifying hypothesis that illuminates both the effects of the mutation and physiological signaling pathways. R58Q promotes an OFF state of the thick filaments that reduces the number of myosin head domains that are available for actin interaction and ATP utilization. Moreover this mutation uncouples two aspects of length-dependent activation (LDA), the cellular basis of the Frank-Starling relation that couples cardiac output to venous return; R58Q reduces maximum calcium-activated force with no significant effect on myofilament calcium sensitivity. Finally, phosphorylation of R58Q-RLC to levels that may be relevant both physiologically and pathologically restores the regulatory state of the thick filament and the effect of sarcomere length on maximum calcium-activated force and thick filament structure, as well as increasing calcium sensitivity. We conclude that perturbation of thick filament-based regulation may be a common mechanism in the etiology of missense mutation-associated HCM, and that this signaling pathway offers a promising target for the development of novel therapeutics.

1. Introduction

The cardiac cycle of contraction and relaxation is governed by transient interactions between the actin-containing thin and myosin-containing thick filaments, coupled to the hydrolysis of ATP [1]. During systole, activation of the thin filaments via calcium binding to troponin releases tropomyosin from its blocked position, allowing strong interaction between the myosin catalytic domains and their binding sites on actin. Structural re-arrangements in the actin-bound catalytic domains, associated with the release of inorganic phosphate from the active site, are amplified and transferred via the light chain domain (LCD) to the thick filament backbone, leading to nm-scale displacement of the thin filaments towards the center of the sarcomere.

Although calcium binding to and dissociation from the thin filaments are generally regarded as the permissive steps allowing myofilament activation and relaxation, respectively, recent evidence suggested that the structure of the thick filaments is an important determinant of cardiac muscle performance. The concept of a regulatory structural transition in the myosin-containing thick filaments originated from studies on invertebrate skeletal [2] and mammalian smooth muscle [3], but has recently been extended to cardiac muscle. Electron microscopy reconstructions of isolated thick filaments from mammalian cardiac muscle suggest that myosin heads in the OFF state of the thick filament are folded against their tail domains, reducing their availability for actin-binding, ATP hydrolysis and force production [4,5]. Consistent with these structural data, biochemical studies on isolated cardiac muscle preparations demonstrated the existence of a pool of myosin heads in a state with ultra-low ATPase activity in both relaxing and activating conditions, known as the super-relaxed state (SRX) [6]. Regulatory signaling pathways including post-translational modifications of RLC [7] and myosin binding protein-C (cMyBP-C) [8], and mechano-sensing [9] have been suggested to regulate cardiac muscle function by modulating the myosin OFF or SRX state and the number of myosin heads available for contraction.

Although the molecular details of the protein-protein interactions responsible for the OFF state have not been described at the level of

* Corresponding author.
E-mail address: thomas.kampourakis@kcl.ac.uk (T. Kampourakis).

https://doi.org/10.1016/j.yjmcc.2018.02.009
Received 20 November 2017; Received in revised form 10 February 2018; Accepted 12 February 2018
Available online 13 February 2018

high-resolution structures, recent modelling of isolated myosin head domain structures into the EM-derived electron density maps suggests that the OFF state might be stabilized by conserved interactions between the catalytic domains, myosin tails and LCDs of the two-headed myosin molecule [5,10,11]. Subsequent mapping of myosin missense mutations associated with both hypertrophic and dilated cardiomyopathy onto these models suggests that perturbation of intra- and intermolecular interactions associated with the OFF state might be involved in the etiology of these diseases. However, no general paradigm of structure-function relationships for these mutations has been established to date.

The R58Q mutation in the myosin regulatory light chain has frequently been associated with a malignant form of familial hypertrophic cardiomyopathy in different patient cohorts [12–14], causing early onset disease and a high incidence of sudden cardiac death. Previous studies that attempted to characterize the effects of the R58Q mutation on cardiac muscle function have led to somewhat conflicting results in terms of its effect on force development and ATPase activity [15–17], most likely associated with the different preparations and experimental protocols employed. *In vivo* analysis of transgenic mouse models expressing human RLC carrying the R58Q mutation showed severe diastolic dysfunction [18], consistent with the hypertrophic phenotype observed in human gene mutation carriers. However, the molecular basis of R58Q's functional effects has mainly been studied using isolated proteins, leading to diverse proposals that cardiac muscle dysfunction might be due to decreased calcium binding to RLC [19], altered load-dependent kinetics [20] or decreased intrinsic force production by myosin [21].

Here we show that the wide range of effects of the R58Q mutation can be understood in terms of the structure and regulatory state of the thick filament. We measured structural changes in the thick filaments of rat ventricular trabeculae by polarized fluorescence from bifunctional rhodamine probes on either wildtype RLC or RLCs containing the R58Q mutation, and combined the results from the *in situ* experiments with biochemical studies of isolated myofilament function and protein interactions *in vitro*. We show that R58Q stabilizes the thick filament OFF state associated with reduced contractility and perturbed length-dependent activation of cardiac myofilaments. We also show that thick filament activation by RLC phosphorylation counteracts the effects of the mutation. Because myofilament desensitization associated with RLC dephosphorylation has been commonly observed in heart failure [22,23], thick filament activation may offer an attractive new approach for the development of heart failure therapeutics.

2. Materials and methods

2.1. Reagents

The RLC binding site peptide of the human β-cardiac myosin heavy chain encompassing amino acids 805–837 (ERRDSLLVIQWNIRAFMGVKNWPWMKLYFKIK) was purchased from Peptide Protein Research Ltd. (Fareham, PO15 6DP, UK) (> 95% HPLC purity).

2.2. Preparation of bifunctional rhodamine labelled RLC and reconstitution into rat right ventricular trabeculae

Bifunctional sulforhodamine (BSR) labelled RLCs were prepared as previously described [24]. BSR-cRLCs were exchanged into demembranated trabeculae by extraction in CDTA-rigor solution (composition in mmol/L: 5 CDTA, 50 KCl, 40 Tris-HCl, 0.1% (v/v) Triton X-100, pH 8.4) for 30 min followed by reconstitution with 40 μmol/L BSR-cRLC in relaxing solution for 1 h at 22 °C, replacing ~50–70% of the endogenous RLC (see Results). The average maximum calcium activated force after reconstitution with WT-BSR-cRLC-E was 87 ± 3% (mean ± SEM, n = 16) of that before RLC exchange.

2.3. Fluorescence polarization experiments

Activation protocols and composition of experimental solutions were identical to those described previously for fluorescence polarization experiments [24,25]. Polarized fluorescence intensities were measured as described previously for skeletal and cardiac muscle fibers [25,26]. Trabeculae were mounted between a strain gauge force transducer (KRONEX, Oakland, California 94,602, USA; model A-801, resonance frequency ~2 kHz) and motor (Aurora Scientific, Dublin, D6WY006, Ireland; Model 312C). Fluorescence emission from WT-BSR-cRLC-E and R58Q-BSR-cRLC-E in trabeculae was collected by a 0.25 N.A. objective using an excitation light beam in line with the emission path. The polarization of the excitation and emitted beams was set either parallel or perpendicular to the trabecular axis, allowing determination of the order parameter $< P_2 >$ that describes the dipole orientations in the trabeculae [27]. The sarcomere length of trabeculae was measured by laser diffraction in relaxing solution prior to each activation. Activating solution contained (in mmol/L): 25 imidazole, 15 Na_2CrP, 58.7 KPr, 5.65 Na_2ATP, 6.3 $MgCl_2$, 10 $CaCl_2$, 10 K_2EGTA, 1 DTT, pH 7.1. Each activation was preceded by a 2-min incubation in pre-activating solution (composition in mmol/L: 25 imidazole, 15 Na_2CrP, 108.2 KPr, 5.65 Na_2ATP, 6.3 $MgCl_2$, 0.2 K_2EGTA, 1 DTT, pH 7.1). Solutions with varying concentrations of free [Ca^{2+}] were prepared by mixing relaxing and activating solutions using MAXCHELATOR software (maxchelator.stanford.edu). Isometric force and steady-state fluorescence polarization values were measured once steady force had been established. The dependence of force and order parameters on free calcium concentration was fitted to data from individual trabeculae using non-linear least-squares regression to the modified Hill equation:

$$F = Y_0 + A \times ([Ca^{2+}]^{n_H}/(-\log_{10}[pCa_{50}]^{n_H} + [Ca^{2+}]^{n_H}))$$

where pCa_{50} is the negative logarithm of [Ca^{2+}] corresponding to half-maximal change in F, n_H is the Hill coefficient, Y_0 is the baseline, and A is the amplitude (for normalized force data: $Y_0 = 0$ and $A = 1$). Trabeculae which showed a decline in maximal calcium activated force of > 15% after the pCa titrations were discarded.

The rate of force re-development was measured by a fast release and re-stretch protocol [28]. Briefly, isometrically contracting trabeculae were released by 20% of their initial length (~500 μs step response), held at the new length for ~30 ms, and re-stretched to the original length. The timecourse of force redevelopment was fitted to a single exponential, yielding the rate constant k_{tr}.

2.4. Preparation of cardiac myofibrils and ATPase activity measurements

Cardiac myofibrils (CMFs) were prepared by homogenising freshly frozen ventricular tissue samples in myofibril buffer (composition in mmol/L: 20 imidazole, 75 KCl, 2 $MgCl_2$, 2 EDTA, 1 DTT, 1% (v/v) Triton X-100, pH 7.4, protease inhibitor cocktail (ROCHE Diagnostics Ltd., RH15 9RY, United Kingdom), PhosStop cocktail (ROCHE)) followed by centrifugation at 5000*g* for 5 min at 4 °C. CMFs were washed and homogenised three more times in the same buffer without Triton X-100. Endogenous RLCs were extracted from CMFs and reconstituted with recombinant proteins as described previously [19]. For ATPase measurements CMFs were washed three times in ATPase assay buffer (composition in mmol/L: 20 MOPS, 35 NaCl, 5 $MgCl_2$, 1 EGTA, 1 DTT, pH 7.0) with varying concentrations of $CaCl_2$ (pCa 9 to pCa 4.3) and the CMF concentration adjusted to 0.5 mg/mL. Reactions were started by the addition of 2.5 mmol/L ATP and samples taken at the indicated time points were quenched with 0.5 volumes ice cold 25% (w/v) TCA solution. Samples were kept on ice at all times, diluted with double-deionized water and inorganic phosphate content measured using the malachite green assay according to manufacturer's instructions (SIGMA, GILLINGHAM SP8 4XT, United Kingdom; MAK030).

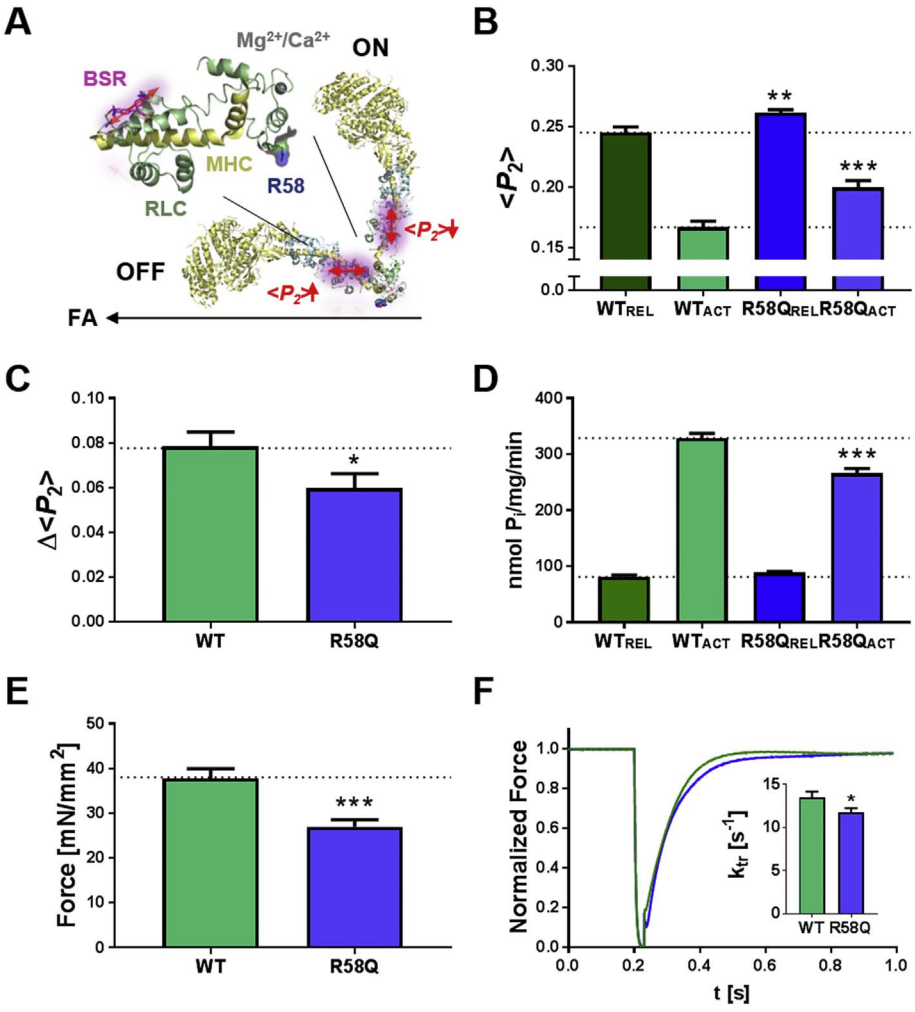

Fig. 1. R58Q stabilizes the OFF conformation of the myosin heads. (A) *Left:* Structure of the RLC-region of myosin with RLC and myosin heavy chain (MHC) shown in green and yellow, respectively. Arginine 58 is shown in van-der-Waals representation, and the BSR probe attached to the E-helix and putative Ca^{2+}/Mg^{2+} binding site are shown in purple and grey, respectively. *Right:* OFF and ON orientations of the myosin heads with respect to the filament axis (FA; black arrow), reported by parallel (high value of the order parameter $< P_2 >$) and perpendicular (low $< P_2 >$) orientations of the E-helix probe, respectively. (B) $< P_2 >$ measured from WT- (green) and R58Q-BSR-cRLC-E (blue) exchanged ventricular trabeculae in relaxing conditions (REL, pCa 9) and full calcium activation (ACT, pCa 4.3) at ~1.9 μm sarcomere length. (C) Decrease in $< P_2 >$ ($\Delta < P_2 >$) on calcium activation for WT- and R58Q-BSR-cRLC-E exchanged trabeculae. (D) ATPase activity of cardiac myofibrils in relaxing conditions and full calcium activation exchanged with either WT- (green) or R58Q-RLC (blue). (E) Maximum isometric force and (F) rate of force re-development of WT- and R58Q-BSR-cRLC-E exchanged ventricular trabeculae. Means ± SEM (n = 4–16). Statistical significance of difference between WT and R58Q groups was assessed with a two-tailed unpaired Student's *t*-test: *p < .05, **p < .01, ***p < .001. (For interpretation of the references to colour in this figure legend, the reader is referred to the web version of this article.)

2.5. RLC phosphorylation in vitro and in situ

In vitro kinase assays for RLCs were performed in cMLCK assay buffer (composition in mmol/L: 25 HEPES, 50 NaCl, 2 $MgCl_2$, 1 $CaCl_2$, 2 DTT, 1 ATP, pH 7) in a total volume of 50 μL containing 0.5 mg/ml (~25 μmol/L) RLC as substrate. Calmodulin was added to a final concentration of 6 μg/mL. The reactions were started by adding the C-terminal fragment of cMLCK to a final concentration of 0.2 μmol/L. The reactions were incubated for 30 min at 30 °C, quenched with 5× sample buffer containing 10 M urea, and analyzed by urea-glycerol-PAGE.

RLC-exchanged cardiac myofibrils (0.5 mg/mL) were phosphorylated *in situ* in activating solution (pCa 4.3) containing 25 μmol/L Blebbistatin and 6 μg/ml calmodulin. Reactions were started by addition of cMLCK fragment to a final concentration of 0.2 μmol/L and incubated at 30 °C. Samples were taken at the indicated time points, myofibrils harvested by centrifugation and solubilized in SDS-PAGE loading buffer. RLCs were phosphorylated in demembranated trabeculae as previously described [7]. Briefly, trabeculae were incubated in relaxing buffer (pCa 9) containing 30 mmol/L 2,3-butadione monoxime (BDM), washed in activating solution (pCa 4.3) containing 30 mmol/L BDM and then incubated in activating solution (pCa 4.3) containing 30 mmol/L BDM, 1 μmol/L cMLCK and 1 μmol/L CaM. After 1 h, BDM, cMLCK and CaM were removed from the trabeculae by three washes in relaxing solution for 10 min. RLC phosphorylation levels were analyzed by Phostag™-SDS-PAGE followed by Western blot against RLC as described previously [7].

2.6. Reconstitution of recombinant RLCs into isolated β-cardiac myosin, and F-actin activated ATPase measurements

Isolated porcine β-cardiac myosin (Cytoskeleton Inc., Denver, CO 80223, USA; MYO3-A) was depleted of its endogenous RLCs and reconstituted with recombinant RLCs as described previously [21]. Rabbit skeletal actin was purchased from Sigma (A2522), and further purified by de-polymerization in general actin buffer (composition in mmol/L: 5 Tris-HCl, 0.2 $CaCl_2$, 0.2 ATP, 0.5 DTT, pH 8.0) followed by centrifugation at 15000 g for 15 min at 4 °C. F-actin was re-polymerized by addition of 10% (v/v) polymerization buffer (composition in mmol/L: 500 KCl, 20 $MgCl_2$, 10 ATP) for 1 h at 22 °C. F-actin was pelleted by centrifugation at 100,000 g for 1 h at 4 °C and re-suspended in assay buffer for ATPase measurements. As a control, pre-formed F-actin filaments were purchased from Cytoskeleton Inc. (AKF99). Both F-actin preparations gave identical results. F-actin activated ATPase activity of RLC-exchanged myosin (0.1 mg/mL final concentration) was measured in 25 mmol/L imidazole pH 7.0, 3 mmol/L $MgCl_2$, 30 mmol/L KCl and 1 mmol/L DTT. Reactions were started by adding 2.5 mmol/L ATP and incubated for 30 min at 30 °C. Reactions were quenched with 0.5 volumes of ice cold 25% (w/v) TCA, diluted with ddH_2O and debris removed by centrifugation at 15000 g for 30 min. The rate of phosphate release was measured with the malachite green method as described previously [29].

2.7. Microscale thermophoresis

Microscale thermophoresis experiments were performed on a

Monolith NT.115 instrument (NanoTemper, Cambridge CB3 0AX, United Kingdom) in interaction buffer containing 20 mmol/L MOPS pH 7, 1 mmol/L $MgCl_2$, 50 mmol/L KCl, 1 mmol/L DTT and 0.05% (v/v) Tween-20. WT- and R58Q-RLCs were labelled with Alexa 647-NHS (Molecular Probes Inc., Thermo Fischer Scientific, Paisley, PA4 9RF, United Kingdom) according to manufacturer's instructions, and dye incorporation confirmed by HPLC and ESI-mass spectrometry. All proteins were either gel-filtered into and/or extensively dialysed against interaction buffer. Titration experiments were performed with a fixed Alexa 647 - RLC concentration of 200 nmol/L in standard treated capillaries.

3. Results

3.1. R58Q stabilizes the OFF conformation of the myosin heads

We used polarized fluorescence from a bifunctional sulforhodamine (BSR) probe attached to the RLC E-helix (Fig. 1A) to determine the effects of the R58Q mutation on myosin head conformation in demembranated rat right ventricular trabeculae with an endogenously low level of RLC phosphorylation (< 0.05 mol P_i/mol RLC) [30]. The E-helix labelling site in the C-lobe was chosen to avoid any direct effects of probe attachment and R58Q mutation on the structure of the N-lobe. The RLC E-helix is roughly parallel to the myosin lever arm, and provides a sensitive and reproducible signal for the orientation of the RLC-region of myosin with respect to the thick filament axis. BSR-RLCs were introduced into demembranated trabeculae by an extraction-reconstitution protocol (see Materials and Methods), replacing 69 ± 3% (mean ± SEM, n = 5) of the native RLCs as estimated by SDS-PAGE and Western blot against RLC (Fig. S1A). Localization of BSR-labelled R58Q-RLCs to the sarcomeric A-band was confirmed by counter-stain against myosin heavy chain and confocal microscopy (Fig. S1B). Polarized fluorescence intensities were used to calculate the order parameter $< P_2 >$, which is equal to +1 if the E-helix is parallel to the thick filament axis and −0.5 if it is perpendicular (Fig. 1A).

$< P_2 >$ for the wildtype RLC E-helix probe (WT-BSR-cRLC-E) is reduced from ~0.25 to ~0.16 on calcium activation of ventricular trabeculae (Fig. 1B), indicating a more perpendicular orientation of the myosin heads with respect to the thick filament, consistent with previous results [29]. $< P_2 >$ for the E-helix probe was significantly higher for R58Q than wildtype RLC, both during relaxing conditions (REL, pCa 9) and full calcium activation (ACT, pCa 4.3), suggesting that the R58Q mutation induces a more parallel orientation of the RLC-region of the myosin heads in both conditions. Moreover, the effect was significantly larger for full calcium activation. The decrease in $< P_2 >$ associated with full calcium activation ($\Delta < P_2 >$), a measure of the extent of calcium-dependent thick filament activation (Fig. S2), was ~30% smaller in trabeculae exchanged with R58Q-BSR-cRLC-E (Fig. 1C).

These effects of the R58Q mutation on myosin head conformation were accompanied by functional changes. Although there was no significant effect on the ATPase activity of cardiac myofibrils in relaxing conditions, replacement of 30–40% of endogenous rat ventricular RLC by R58Q-RLC in freshly prepared cardiomyofibrils (CMFs) (Fig. S3) reduced maximal calcium-activated ATPase activity by ~20% with respect to control CMFs exchanged with unlabeled WT-RLC (Fig. 1D), as expected from the more OFF orientation of the myosin head domain inferred from the E-helix probe orientation. The R58Q mutation reduced maximum Ca^{2+}-activated isometric force of ventricular trabeculae by a similar extent (~30%) (Fig. 1E). The rate of force redevelopment (k_{tr}) following a fast release-stretch protocol [28] at full calcium activation was reduced by ~15% with respect to the WT control (Fig. 1F), indicating slower cross-bridge kinetics in the presence of the mutation.

In summary, the R58Q mutation promotes the OFF conformation of the myosin heads on the thick filament, and reduces isometric force, the rate of force redevelopment and myofibrillar ATPase.

3.2. Effects of the R58Q mutation on isolated cardiac myosin and RLC

As a step towards dissecting the molecular mechanism of R58Q's effect on myosin head conformation, we measured the affinity of unlabeled WT- and R58Q-RLC for the cardiac myosin heavy chain (MHC). About 70% of the native RLC was extracted from isolated porcine β-cardiac myosin and the depleted myosin reconstituted with different mole fractions of either WT- or R58Q-RLC. The K_d for RLC binding was estimated as ~4 μmol/L for both RLCs by densitometric analysis using the ELC as an internal loading control, in agreement with previous results [31], suggesting that R58Q does not affect the RLC-MHC interaction (Fig. S4A). We also titrated a short MHC peptide corresponding to the RLC binding site against either WT or R58Q-RLC and found that tryptophan fluorescence from the peptide increased by about 80% upon RLC binding for both WT and R58Q (Fig. S4B). This result suggests that the tryptophan residues are in a similar chemical environment, but the apparent dissociation constant for the RLC-MHC peptide complex was too low (< 0.5 μmol/L) to be measured reliably using this approach.

We further assessed the effect of the RLC R58Q mutation on the function of isolated myosin by steady-state acto-myosin ATPase measurements. RLC depleted β-cardiac myosin was fully reconstituted with either WT- or R58Q-RLC, or a mixture of both (Fig. 2A), and the dependence of the myosin ATPase activity on the F-actin concentration fitted to the Michaelis-Menten equation (Fig. 2B). V_{max} did not significantly differ among the three groups (~6 s^{-1} $head^{-1}$), but K_M increased from 1.50 ± 0.08 μmol/L (mean ± SEM, n = 3) for myosin exchanged with WT-RLC to 2.91 ± 0.06 μmol/L for myosin exchanged with R58Q-RLC, suggesting that the R58Q mutation decreases the probability of actin-myosin interaction *in vitro*. Myosin exchanged with a mixture of WT- and R58Q-RLC showed an intermediate value of K_M. These results are consistent with the *in situ* experiments in demembranated trabeculae, giving further support for the conclusion that R58Q stabilizes the OFF conformation of the myosin molecule. The effect of the R58Q mutation on RLC stability was assessed by Microscale Thermophoresis (MST) in the presence of increasing concentrations of guanidine hydrochloride (GdnHCl) (Fig. 2C; Fig. S5A). Both Alexa 647 labelled WT- and R58Q-RLCs showed a biphasic unfolding behavior, with the MST signal decreasing between 0 mol/L and 3 mol/L GdnHCl before increasing again at [GdnHCl] > 3 mol/L. Although the thermophoretic mobilities of the two RLCs in the presence of 8 mol/L GdnHCl were indistinguishable, the MST signal of R58Q-RLC in the absence of GdnHCl was significantly larger than that of WT-RLC suggesting a different protein conformation. Data points between 0 and 3 mol/L GdnHCl were fitted to a Hill equation resulting in Hill coefficients > 2, suggesting a cooperative unfolding mechanism, with EC_{50} values of 1.28 ± 0.11 mol/L (mean ± SEM, n = 3) and 0.79 ± 0.10 mol/L for WT-RLC and R58Q-RLC, respectively, indicating lower RLC stability in the presence of R58Q.

RLC can also bind to N-terminal domains of cardiac myosin binding protein-C (cMyBP-C) [10,32] and this interaction may influence the conformation of the myosin heads in native thick filaments. We therefore determined the affinity of both the WT- and R58Q-RLC for different domains of cMyBP-C using MST (Fig. 2D and Fig. S5B). Isolated WT-RLC binds to a cMyBP-C fragment spanning domains C0 to C2 (C0C2) with a K_d of 8.6 ± 0.1 μmol/L (mean ± SEM, n = 6), but does not interact with a fragment of the central domains (C3C5), suggesting a specific interaction with the N-terminus of cMyBP-C. The isolated RLC retained an interaction with C0C2 in the presence of the R58Q mutation, albeit with a slightly decreased affinity (K_d of 9.7 ± 0.7 μmol/L, n = 4).

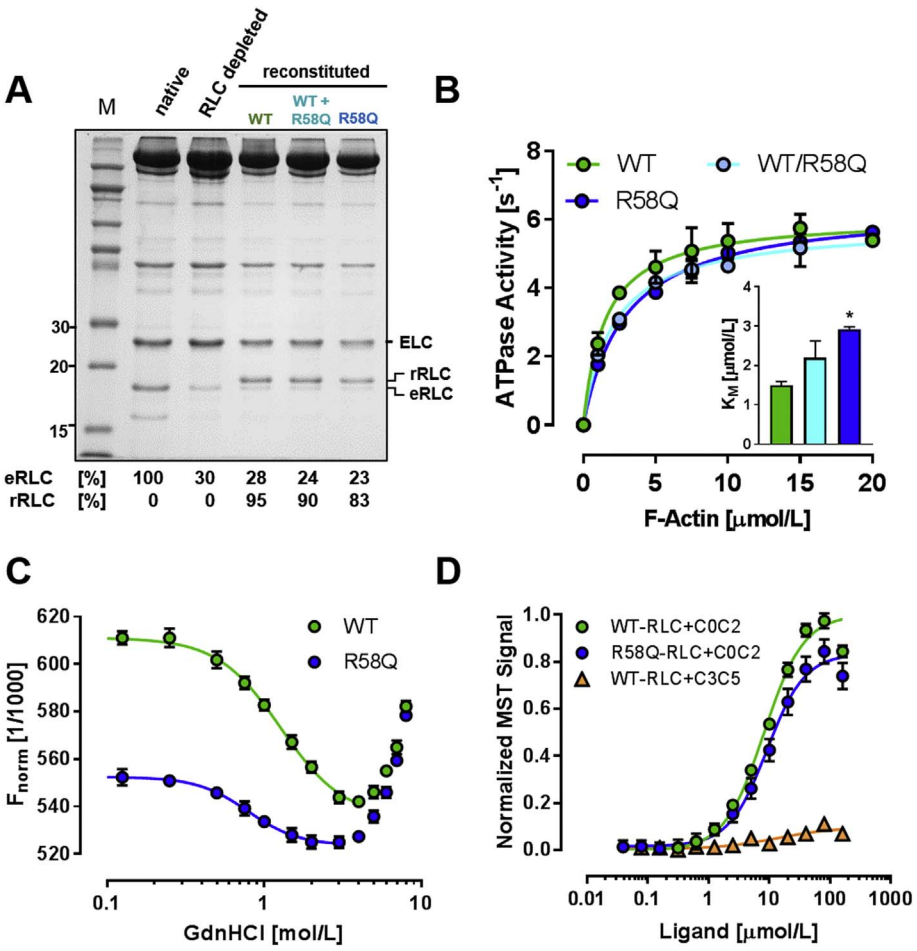

Fig. 2. Effects of R58Q mutation on isolated cardiac myosin and RLC. (A) SDS-PAGE of RLC-depleted porcine β-cardiac myosin, and myosin reconstituted with either WT- and/or R58Q-RLC. The endogenous (eRLC) and recombinant RLC (rRLC) are labelled accordingly. (B) F-actin dependent ATPase activity of RLC-exchanged β-cardiac myosins from (A) (for details see Materials and Methods). Data points fitted to the Michaelis-Menten equation (solid lines). (C) Protein stability of WT- and R58Q-RLCs were assessed by Micro-scale Thermophoresis (MST) against increasing concentrations of Guanidine Hydrochloride (GdnHCl). Data points between 0 and 3 mol/L GdnHCl were fitted to a Hill equation (solid lines). (D) Binding of WT- and R58Q-RLC to N-terminal (C0C2) domains of cMyBP-C assessed by MST. Means ± SEM (n = 4–6 for C0C2; n = 1 for C3C5).

3.3. R58Q perturbs the effect of sarcomere length on maximum force but not that on calcium sensitivity

Since changes in the conformation of the myosin heads may be involved in length-dependent activation (LDA) in cardiac muscle and the Frank-Starling Law of the heart [7,33,34], and impaired LDA has been linked to heart failure associated with sarcomeric protein missense mutations [35], we investigated the effect of the R58Q mutation on the change in myosin head conformation associated with LDA.

Ventricular trabeculae were exchanged with either WT- or R58Q-BSR-cRLC-E, and the [Ca^{2+}]-dependence of force development and myosin head orientation determined at short (~1.9 μm) and long (~2.2 μm) sarcomere lengths (Fig. 3; Table S1). Both WT- and R58Q-BSR-cRLC-E exchanged trabeculae showed a significant increase in the calcium sensitivity of force on increasing sarcomere length (SL). The calcium concentration corresponding to half-maximal force (pCa_{50}) increased by 0.11 ± 0.01 and 0.12 ± 0.02 pCa units (mean ± SEM, n = 4–7) for the WT and R58Q groups, respectively, indicating that the R58Q mutation had no detectable effect on the increase in myocardial calcium sensitivity with increase in sarcomere length (Fig. 3A and B; Table S1).

Both passive (measured at pCa 6.4) and active force (measured at pCa 4.3) significantly increased with increasing sarcomere length in trabeculae exchanged with WT-BSR-cRLC-E (Fig. 3C). Active isometric force increased by ~25%, from 34.8 ± 2.3 to 43.6 ± 4.4 mN/mm^2 (mean ± SEM, n = 6). However, the length-dependence of active force was almost abolished in the presence of R58Q-RLC (it was only ~6%, from 26.9 ± 2.6 to 28.9 ± 2.9 mN/mm^2). Passive force at each sarcomere length was the same in the WT and R58Q groups (Fig. 3D; Table S1).

Increasing SL from 1.9 to 2.2 μm increased $< P_2 >$ and the calcium sensitivity of the $< P_2 >$-pCa relation by 0.14 ± 0.04 and 0.13 ± 0.02 pCa units for WT- and R58Q-BSR-cRLC-E exchanged trabeculae, respectively (Figs. 3E and F; Table S1). Moreover, the effect of the R58Q mutation on the orientation of the myosin head domains in relaxing conditions is smaller at longer sarcomere length. However, the amplitude of the structural change associated with activation ($\Delta < P_2 >$) was almost independent of SL in the presence of R58Q, in contrast with the ~24% change in the WT group. These effects on the structure of the thick filament are strikingly similar to those on active isometric force, suggesting that the higher active force at the longer SL is associated with a more ON structure of the thick filament [34], and that both effects are abolished by the R58Q mutation.

3.4. RLC phosphorylation increases active force and restores the effect of SL on active force in R58Q-RLC exchanged trabeculae

RLC phosphorylation increases the contractility of cardiac muscle by promoting the thick filament 'ON' state characterized by a more perpendicular orientation of the myosin heads with respect to the thick filament axis [7,30]. Since these effects are in the opposite direction to those produced by the R58Q mutation, we hypothesized that phosphorylation of RLC might restore myosin conformation and function in R58Q-RLC exchanged trabeculae.

First we used an expressed cardiac myosin light chain kinase (cMLCK) to determine whether the R58Q mutation interferes with RLC phosphorylation. Both WT- and R58Q-RLCs could be fully phosphorylated by cMLCK *in vitro* (Fig. 4A), consistent with previously published results using smooth muscle MLCK [19]. Next we measured the time course of *in situ* phosphorylation of RLCs in cardiac myofibrils

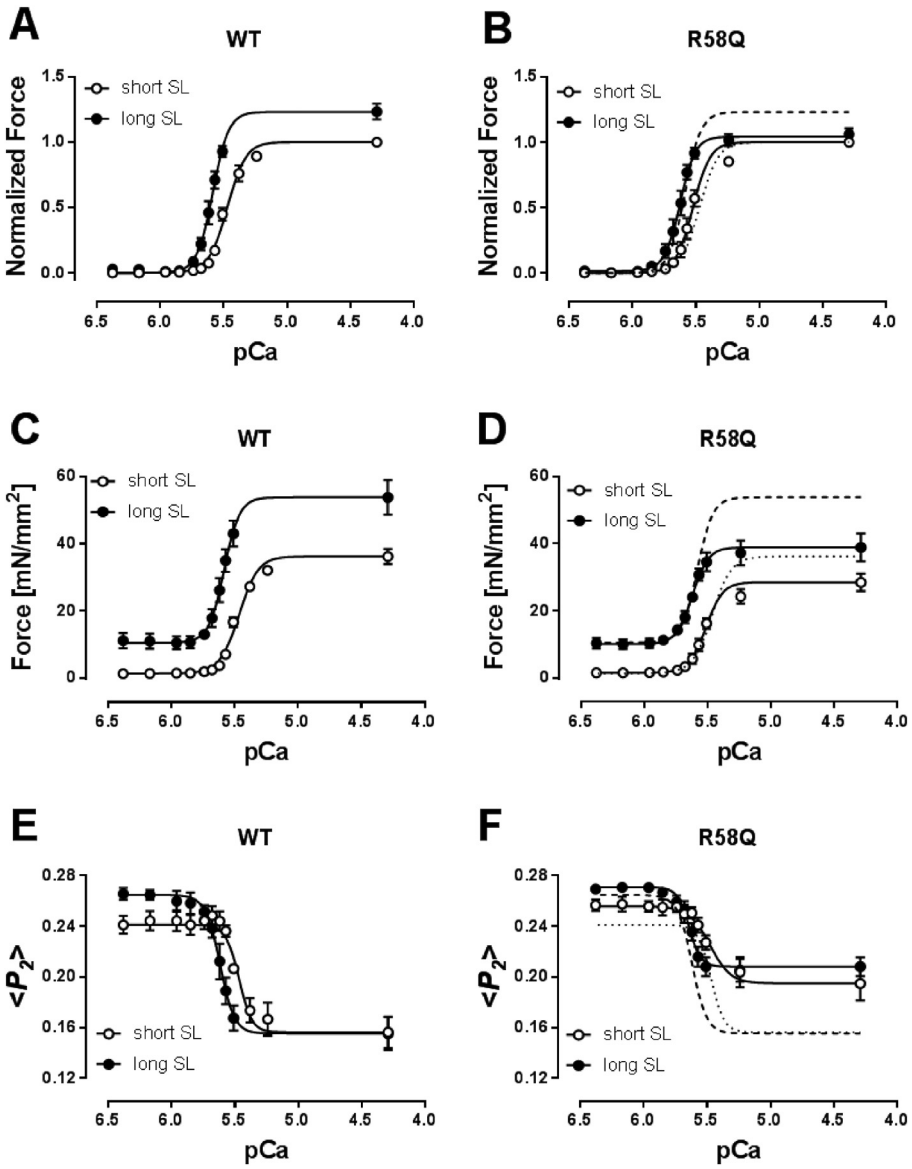

Fig. 3. R58Q perturbs the effect of sarcomere length on maximum force but not that on calcium sensitivity of cardiac trabeculae. Normalized (A and B) and absolute (C and D) force-pCa relations of WT- (A and C) and R58Q-BSR-cRLC-E (B and D) exchanged trabeculae at short (~1.9 μm) and long (~2.2 μm) sarcomere length. Force is normalized to maximum force at 1.9 μm sarcomere length. $< P_2 >$ -pCa relations for WT- and R58Q-BSR-cRLC-E exchanged trabeculae measured in parallel with force are shown in (E) and (F), respectively. Dashed and dotted lines in (B), (D) and (F) denote Hill fits for WT-BSR-cRLC-E exchanged trabeculae at short and long sarcomere length, respectively. Means ± SEM (n = 4–7).

containing ~50% of either WT- or R58Q-RLC (Fig. 4B). In contrast to trabeculae, myofilaments in CMFs are directly accessible by the kinase and allow direct comparison of the rate of RLC phosphorylation. RLCs in both groups could be phosphorylated to over 90% within 90 min with a similar time course (Fig. 4C), confirming the results with isolated RLCs. Double exponential fitting suggested that these phosphorylation time courses have slow and fast components of almost equal amplitude. Control experiments with native untreated CMFs showed only the slow component (Fig. 4C, triangles), perhaps indicating selectivity of the human cMLCK for human RLCs.

Incubation of RLC-exchanged trabeculae with Ca^{2+}/CaM/cMLCK for 1 h increased the *in situ* phosphorylation level of exchanged R58Q-BSR-cRLC-E and total RLCs to 0.27 ± 0.03 mol Pi/mol RLC and 0.29 ± 0.04 molPi/mol RLC (mean SEM, n = 7) respectively, indicating that native rat and R58Q-BSR-cRLC-E were phosphorylated equally by cMLCK (Fig. S6).

Consistent with our previous study using a BSR probe attached to the RLC N-lobe [7], RLC phosphorylation to ~0.3 mol P_i/mol RLC (Fig. S6) of R58Q-BSR-cRLC-E exchanged trabeculae increased the calcium sensitivity of force by ~0.07 pCa units (Fig. S7A) and increased maximum active isometric force by ~30%, from ~24 to ~31 mN/mm^2. The latter value is close to that of WT-BSR-cRLC-E exchanged trabeculae in the RLC dephosphorylated state at the same sarcomere length (Fig. 4D, dotted line).

Phosphorylation of RLC to ~0.3 mol P_i/mol RLC (Fig. S6) by cMLCK also increased the extent of calcium-induced activation of the thick filament as measured by $\Delta < P_2 >$ from the RLC E-helix probe, to values close to those obtained for unphosphorylated WT-BSR-cRLC-E (Fig. 4E, dotted lines), and increased the rate of force redevelopment (k_{TR}) from ~12 s^{-1} to ~18 s^{-1} (compared to ~14 s^{-1} for WT BSR-cRLC-E) (Fig. 4F). These results indicate that RLC phosphorylation restores cardiac contractility and the regulatory state of the thick filament in the presence of the R58Q mutation.

Incubation of R58Q-RLC exchanged trabeculae with cMLCK also restored the dependence of maximum active force on sarcomere length. Maximum active force of R58Q-BSR-cRLC-E exchanged trabeculae *after* RLC phosphorylation to ~0.3 mol P_i/mol RLC (Fig. S6) increased by ~28% on increasing sarcomere length from 1.9 to 2.2 μm (compared to

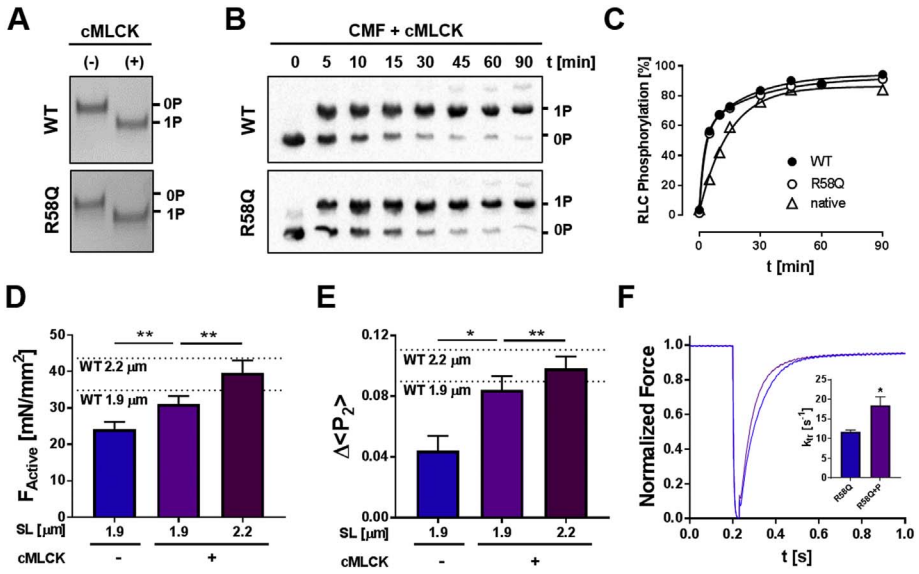

Fig. 4. RLC phosphorylation restores myofilament function in the presence of R58Q-RLC. (A) *In vitro* kinase assay of WT- and R58Q-RLC incubated without (−) and with cMLCK (+) and analyzed by urea-glycerol PAGE. (B) *In situ* phosphorylation of WT- and R58Q-RLC exchanged into cardiac myofibrils (CMF) analyzed by Phostag™-SDS-PAGE and Western blot against RLC. (C) Time-course of phosphorylation of native, and WT- and R58Q-RLC exchanged CMFs. (D) Active isometric force (F_{Active}) and (E) $\Delta < P_2 >$ of R58Q-BSR-cRLC-E exchanged trabeculae before (−) and after RLC phosphorylation (+) to ~0.3 mol P_i/mol RLC (Fig. S6) at short sarcomere length (~1.9 µm), and after RLC phosphorylation at long sarcomere length (~2.2 µm). The values obtained for WT-BSR-cRLC-E at each sarcomere length are indicated by dotted lines and labelled accordingly. (F) Rate of force re–development of R58Q-BSR-cRLC-E exchanged trabeculae before (blue) and after RLC phosphorylation (purple). Means ± SEM (n = 4–7). Statistical significance of differences of values were assessed with a two-tailed paired Student's t-test: *p < .05, **p < .01. (For interpretation of the references to colour in this figure legend, the reader is referred to the web version of this article.)

only ~6% *before* RLC phosphorylation), similar to the ~25% increase observed for unphosphorylated WT-BSR-cRLC-E (Fig. 4D, dotted lines). RLC phosphorylation preserved the increase in calcium sensitivity of force associated with LDA (ΔpCa_{50} of ~0.1), but decreased the Hill coefficient of the force-calcium relation from ~6 to ~4 (Fig. S7B), as reported previously [7]. Similar to the effects on maximum active force, $\Delta < P_2 >$ measured from R58Q-BSR-cRLC-E increased by ~20% on sarcomere stretch in the presence of phosphorylated RLCs (Fig. 4E) indicating a higher fraction of heads in the perpendicular orientation. In summary, RLC phosphorylation counteracts the effects of R58Q on thick filament activation and force development, and restores the regulatory state of the thick filament in the presence of this mutation.

4. Discussion

4.1. RLC R58Q stabilizes the OFF state of the thick filament

The present results suggest that the HCM-associated mutation R58Q in the myosin RLC disrupts the function of cardiac muscle by interfering with the thick filament-based regulatory system that operates in parallel with the canonical calcium/thin filament system (Fig. 5). *In situ* fluorescence polarization measurements from a bifunctional probe on the E-helix of the RLC in ventricular trabeculae indicated a more parallel orientation of the myosin head domains with respect to the thick filament in the presence of R58Q, as shown by a higher value of the order parameter $< P_2 >$ in relaxing conditions, although the effect is diminished at long sarcomere length. This higher value of $< P_2 >$ for the E-helix probe is characteristic of the 'interacting heads motif' (IHM) conformation of myosin associated with the OFF state of the thick filament (Fig. 1A).

The R58Q mutation also reduced the changes in orientation of the RLC-region of the myosin heads on calcium activation that are associated with release of myosin heads from the parallel or OFF state close to the surface of thick filament, indicating that a smaller fraction of myosin heads are available for actin binding and force generation in the presence of the mutation. Active force and ATP utilization were reduced to a similar extent [16] as this structural signal, indicating that the R58Q mutation acts by decreasing the number of myosin motors available for contraction rather than by altering motor function *per se*.

The RLC region of the myosin head is involved in many different molecular interactions in the sarcomere, and the present results help to clarify which of these interactions are perturbed by the R58Q mutation. In contrast with previous suggestions that a loss of regulatory

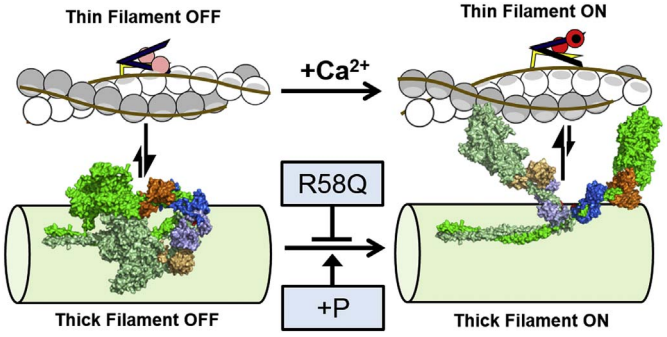

Fig. 5. Model for the effect of R58Q on myofilament activation in the heart. Cardiac contraction is controlled by regulatory structural transitions in both actin-containing thin and myosin-containing thick filaments. During diastole (left) both thin and thick filament are in the OFF state. Tropomyosin (brown lines) blocks myosin-binding sites on actin (white and grey circles), and myosin head domains (space filling representation, green) are sequestered on the surface of the thick filament backbone. During systole (right) calcium (black circle) binds to troponin C (red) and activates the thin filaments by removing inhibitory interactions of troponin I (yellow) and troponin T (purple) with actin, followed by tropomyosin moving azimuthally away from myosin-binding sites on actin. Calcium activation of the thin filament activates myosin heads through so far unknown mechanisms (indicated by vertical arrows), resulting in release of the heads from the surface of the thick filament to become available for actin binding and force-generation. The R58Q mutation in the myosin RLC (blue) reduces cardiac contractility by stabilizing the thick filament OFF state and preventing myosin heads from leaving the thick filament surface. RLC phosphorylation (+P) restores thick filament activation in the presence of the R58Q mutation by destabilizing the OFF state and promoting the myosin head ON state. Homology models for human β-cardiac myosin were created by the Spudich laboratory (http://spudlab.stanford.edu/homology-models/). (For interpretation of the references to colour in this figure legend, the reader is referred to the web version of this article.)

interactions between myosin and cMyBP-C might be associated with the development of HCM [10,32,36], we found no effect of the R58Q mutation on the affinity of isolated RLC for the N-terminal domains of cMyBP-C (Fig. 2D). We also found that the high cooperativity of thick filament calcium activation indicated by a Hill coefficient of around 7 for the $< P_2 >$ -pCa relation is preserved in the presence of the mutation (Table S1), indicating that cooperative interactions between myosin heads in the OFF state are not affected by R58Q. The affinity of RLC for cardiac β-myosin is also not affected by the R58Q mutation (Fig. S4A), suggesting that the interactions between the RLC and the myosin heavy chain and ELC are preserved. The R58Q mutation does not affect the maximum acto-myosin ATPase activity, although it

reduces the K_M, consistent with the *in situ* indication that fewer myosin heads are available for actin interaction, but the properties of the available heads are normal.

On the basis of the present results, the most likely molecular interpretation for the effects of the R58Q mutation would seem to be disruption of intra-molecular interactions within the myosin molecule. R58Q alters the conformation of isolated RLC, destabilizing its tertiary fold (Fig. 2C). These changes could perturb interactions between the two light chain domains of individual myosin molecules, or between its head and tail domains. Since the folded OFF state has also been observed for isolated cardiac myosin [37], such a mechanism might also explain the reduced force and power output of isolated R58Q-RLC exchanged cardiac myosin [20,21]. Our previous fluorescence polarization studies demonstrating distinct conformations of the RLC N- and C-lobes in relaxed and active cardiac muscle [24] are also consistent with this type of mechanism, in which flexibility within the RLC is required for the regulatory transition in myosin. The location of the RLC N-lobe at the junction between the two myosin heads with the tail is well-placed to control regulatory changes in the conformation of the myosin head domains [30].

4.2. R58Q perturbs the effect of sarcomere length on maximum force but preserves its effect on calcium sensitivity

The molecular mechanisms underlying the Frank-Starling Law of the heart and its cellular analogue, length-dependent activation (LDA), remain poorly understood. Recently it has been suggested that thick filament regulation may play a role in LDA, *i.e.* that a more ON state of the thick filament at longer sarcomere length might make more myosin heads available for actin interaction [7,9,33]. Specifically, increased sarcomere length generates mechanical stress that is communicated to the thick filament by the titin links between the tips of the thick filaments and the ends of the sarcomere, which switches the thick filaments ON by a direct mechano-sensing mechanism [7,9,38]. This transition in the thick filaments might then be communicated to the thin filaments by some unknown mechanism. It has also been suggested that two aspects of LDA, the higher force at maximal calcium activation and the change in calcium sensitivity at submaximal calcium, might be mediated by different mechanisms [34], with the former being most directly linked to the regulatory state of the thick filament.

Consistent with that hypothesis, we found that the RLC R58Q mutation had no effect on the sarcomere length-dependence of passive force or the calcium sensitivity of active force, but almost abolished the sarcomere length-dependence of maximum force (Fig. 3). The same distinction between these two aspects of LDA was observed for the regulatory state of the thick filament as reported by the RLC E-helix probe. In terms of the mechano-sensing hypothesis of thick filament regulation, additional passive stress is still transmitted to the thick filaments at longer sarcomere length in the presence of the R58Q mutation, but no longer leads to more myosin heads being released from the thick filament backbone. Thus the R58Q mutation seems to uncouple thick filament stress from its regulatory state, although the effect of sarcomere length on calcium sensitivity is retained, presumably because it is mediated by a separate signaling pathway that links the regulatory states of the thick and thin filaments [33,34].

The present results further suggest that inter-filament signaling is not mediated by the number of myosin heads available for thin filament binding [33,34], since this number becomes almost independent of sarcomere length in the presence of the R58Q mutation. It seems more likely that that inter-filament signaling is mediated by cMyBP-C [24]. The N-terminal domains of cMyBP-C have competing binding sites for both myosin and actin, and N-terminal fragments of cMyBP-C increase the calcium sensitivity of the thin filament in the absence of strong binding myosin heads [24]. Moreover, since the C-terminus of cMyBP-C binds to both the myosin tail and titin, cMyBP-C is ideally positioned to couple the regulatory states of the thick and thin filaments.

4.3. RLC phosphorylation counteracts the effects of the R58Q mutation

The effects of the R58Q mutation on cardiac contractility described above can be counteracted by RLC phosphorylation. R58Q stabilizes the OFF state of the thick filament and the parallel IHM conformation of the myosin heads and decreases contractility, whereas RLC phosphorylation disrupts the OFF state [7,10,30], promotes the ON conformation of the thick filament and increases contractility (Fig. 5). RLC phosphorylation has also been proposed to enhance the function of isolated myosin by increasing either motor stiffness [21] or step size [39]. In terms of thick filament regulatory mechanisms, the antagonistic effects of RLC phosphorylation and R58Q may be related to the role of the RLC region of the myosin heads to control intra-molecular interactions between the two heads of a myosin molecule, and between the heads and the tail domain [10], as discussed in Section 4.1. RLC phosphorylation also restores the sarcomere-length dependence of both active force and the regulatory state of the thick filament in the presence of the R58Q mutation (Fig. 4D,E), presumably by counteracting the stabilization of the OFF state induced by the mutation. cMyBP-C phosphorylation may be able to introduce additional functional effects by perturbing the same signaling pathways [40] through the mechanisms proposed in Section 4.2, and we have previously shown that cMyBP-C is highly phosphorylated in demembranated trabeculae [24].

4.4. Clinical perspective

Although hypertrophic cardiomyopathy mutations are generally associated with hyper-contractility [41], usually associated with an increase in myocardial calcium sensitivity, the R58Q mutation in RLC decreases contractility by stabilizing the OFF state of the thick filament, which may replicate functional defects in early stages of disease development before the clinical manifestation of HCM. Consistent with this hypothesis, decreased cardiac power, output and efficiency has been observed in isolated perfused working hearts from a transgenic mouse model expressing R58Q-RLC [18]. Decreased contractility might lead to HCM by increasing the energy cost of contraction followed by pathogenic remodeling of the heart [42,43], or via hypertrophy acting as a direct compensatory mechanism [44] in later stages of disease progression. It has been suggested that altered phosphorylation of myofilament regulatory proteins could be responsible for the increased calcium sensitivity observed in end-stage heart failure [22], and restoration of phosphorylation levels by an exogenous kinase restored myofilament calcium sensitivity [35], suggesting that hypo-phosphorylation of protein targets and not missense mutations *per se* are responsible for the hyper-contractile phenotype normally associated with HCM. Alternatively, perturbed LDA and mechano-sensing have been implicated as common mechanisms that may contribute to cardiac dysfunction observed in missense gene mutation carriers [35]. Consistent with that hypothesis, the HCM-associated mutation R58Q decreases contractility and sarcomere-length dependent myofilament activation in a RLC phosphorylation-dependent manner. Moreover, reduced levels of RLC phosphorylation have been found in both human end-stage failing myocardium [22], and myocardium from a transgenic mouse model carrying the RLC-R58Q mutation [18], suggesting that RLC dephosphorylation further contributes to cardiac dysfunction and remodeling.

Modulation of cardiac myosin function is a promising route for the development of novel heart failure therapeutics, and much effort has been directed towards the development of small molecule effectors that directly target the myosin head domain [45,46]. An alternative approach, however, would be to modulate the function of cardiac myosin by targeting the normal signaling pathways that control thick filament structure. RLC phosphorylation has been shown to be an important determinant of cardiac muscle function in both health and disease [47,48], and pseudo-phosphorylation of RLC in mouse models carrying sarcomeric protein missense mutations prevents the clinical onset of

HCM [49]. Consistent with these observations, increasing the RLC phosphorylation level in our experiments significantly increased contractility and improved LDA in the presence of the R58Q mutation. Although the signaling pathways upstream of cMLCK are incompletely understood, it may be possible to identify small molecules that specifically activate cMLCK, increase contractility and counteract the development of HCM-associated heart failure.

Acknowledgements

We are grateful to the British Heart Foundation for financial support, and Dr. Martin Reese and Birgit Brandmeier for supplying the calmodulin used in this study. We further thank Luke Smith, David Trentham, Mathias Gautel, and Yin-Biao Sun for help and advice.

Funding

This study was supported by a British Heart Foundation project grant (PG/12/52/29713) to MI and Basic Science Intermediate Fellowship (FS/16/3/31887) to TK.

Disclosures

None.

Appendix A. Supplementary data

Supplementary data to this article can be found online at https://doi.org/10.1016/j.yjmcc.2018.02.009.

References

[1] A.M. Gordon, E. Homsher, M. Regnier, Regulation of contraction in striated muscle, Physiol. Rev. 80 (2000) 853–924.
[2] J.L. Woodhead, Atomic model of a myosin filament in the relaxed state, Nature 436 (2005) 1195–1199.
[3] T. Wendt, D. Taylor, K.M. Trybus, K. Taylor, Three-dimensional image reconstruction of dephosphorylated smooth muscle heavy meromyosin reveals asymmetry in the interaction between myosin heads and placement of subfragment 2, Proc. Natl. Acad. Sci. U. S. A. 98 (2001) 4361–4366.
[4] M.E. Zoghbi, J.L. Woodhead, R.L. Moss, R. Craig, Three-dimensional structure of vertebrate cardiac muscle myosin filaments, Proc. Natl. Acad. Sci. U. S. A. 105 (2008) 2386–2390.
[5] H.A. Al-Khayat, R.W. Kensler, J.M. Squire, S.B. Marston, E.P. Morris, Atomic model of the human cardiac muscle myosin filament, Proc. Natl. Acad. Sci. U. S. A. 110 (2013) 318–323.
[6] P. Hooijman, M.A. Stewart, R. Cooke, A new state of cardiac myosin with very slow ATP turnover: a potential cardioprotective mechanism in the heart, Biophys. J. 100 (2011) 1969–1976.
[7] T. Kampourakis, Y.B. Sun, M. Irving, Myosin light chain phosphorylation enhances contraction of heart muscle via structural changes in both thick and thin filaments, Proc. Natl. Acad. Sci. U. S. A. 113 (2016) E3039–47.
[8] R.W. Kensler, R. Craig, R.L. Moss, Phosphorylation of cardiac myosin binding protein C releases myosin heads from the surface of cardiac thick filaments, Proc. Natl. Acad. Sci. U. S. A. 114 (2017) (E1355-E64).
[9] M. Reconditi, M. Caremani, F. Pinzauti, J.D. Powers, T. Narayanan, G.J. Stienen, et al., Myosin filament activation in the heart is tuned to the mechanical task, Proc. Natl. Acad. Sci. U. S. A. 114 (2017) 3240–3245.
[10] S. Nag, D.V. Trivedi, S.S. Sarkar, A.S. Adhikari, M.S. Sunitha, S. Sutton, et al., The myosin mesa and the basis of hypercontractility caused by hypertrophic cardiomyopathy mutations, Nat. Struct. Mol. Biol. 24 (2017) 525–533.
[11] L. Alamo, J.S. Ware, A. Pinto, R.E. Gillilan, J.G. Seidman, C.E. Seidman, et al., Effects of myosin variants on interacting-heads motif explain distinct hypertrophic and dilated cardiomyopathy phenotypes, elife 6 (2017) E24634.
[12] J. Flavigny, P. Richard, R. Isnard, L. Carrier, P. Charron, G. Bonne, et al., Identification of two novel mutations in the ventricular regulatory myosin light chain gene (MYL2) associated with familial and classical forms of hypertrophic cardiomyopathy, J. Mol. Med. (Berl). 76 (1998) 208–214.
[13] Z.T. Kabaeva, A. Perrot, B. Wolter, R. Dietz, N. Cardim, J.M. Correia, et al., Systematic analysis of the regulatory and essential myosin light chain genes: genetic variants and mutations in hypertrophic cardiomyopathy, Eur. J. Hum. Genet. 10 (2002) 741–748.
[14] S. Morner, P. Richard, E. Kazzam, U. Hellman, B. Hainque, K. Schwartz, et al., Identification of the genotypes causing hypertrophic cardiomyopathy in northern Sweden, J. Mol. Cell. Cardiol. 35 (2003) 841–849.
[15] D. Szczesna-Cordary, G. Guzman, S.S. Ng, J. Zhao, Familial hypertrophic cardiomyopathy-linked alterations in Ca^{2+} binding of human cardiac myosin regulatory light chain affect cardiac muscle contraction, J. Biol. Chem. 279 (2004) 3535–3542.
[16] Y. Wang, Y. Xu, W.G. Kerrick, Y. Wang, G. Guzman, Z. Diaz-Perez, et al., Prolonged Ca2+ and force transients in myosin RLC transgenic mouse fibers expressing malignant and benign FHC mutations, J. Mol. Biol. 361 (2006) 286–299.
[17] L. Wang, P. Muthu, D. Szczesna-Cordary, M. Kawai, Diversity and similarity of motor function and cross-bridge kinetics in papillary muscles of transgenic mice carrying myosin regulatory light chain mutations D166V and R58Q, J. Mol. Cell. Cardiol. 62 (2013) 153–163.
[18] T.P. Abraham, M. Jones, K. Kazmierczak, H.Y. Liang, A.C. Pinheiro, C.S. Wagg, et al., Diastolic dysfunction in familial hypertrophic cardiomyopathy transgenic model mice, Cardiovasc. Res. 82 (2009) 84–92.
[19] D. Szczesna, D. Ghosh, Q. Li, A.V. Gomes, G. Guzman, C. Arana, et al., Familial hypertrophic cardiomyopathy mutations in the regulatory light chains of myosin affect their structure, Ca^{2+} binding, and phosphorylation, J. Biol. Chem. 276 (2001) 7086–7092.
[20] M.J. Greenberg, K. Kazmierczak, D. Szczesna-Cordary, J.R. Moore, Cardiomyopathy-linked myosin regulatory light chain mutations disrupt myosin strain-dependent biochemistry, Proc. Natl. Acad. Sci. U. S. A. 107 (2010) 17403–17408.
[21] A. Karabina, K. Kazmierczak, D. Szczesna-Cordary, J.R. Moore, Myosin regulatory light chain phosphorylation enhances cardiac beta-myosin in vitro motility under load, Arch. Biochem. Biophys. 580 (2015) 14–21.
[22] J. van der Velden, Z. Papp, R. Zaremba, N.M. Boontje, J.W. de Jong, V.J. Owen, et al., Increased Ca2+-sensitivity of the contractile apparatus in end-stage human heart failure results from altered phosphorylation of contractile proteins, Cardiovasc. Res. 57 (2003) 37–47.
[23] S.A. Warren, L.E. Briggs, H. Zeng, J. Chuang, E.I. Chang, R. Terada, et al., Myosin light chain phosphorylation is critical for adaptation to cardiac stress, Circulation 126 (2012) 2575–2588.
[24] T. Kampourakis, Z. Yan, M. Gautel, Y.B. Sun, M. Irving, Myosin binding protein-C activates thin filaments and inhibits thick filaments in heart muscle cells, Proc. Natl. Acad. Sci. U. S. A. 111 (2014) 18763–18768.
[25] Y.B. Sun, F. Lou, M. Irving, Calcium- and myosin-dependent changes in troponin structure during activation of heart muscle, J. Physiol. 587 (2009) 155–163.
[26] S.C. Hopkins, C. Sabido-David, U.A. van der Heide, R.E. Ferguson, B.D. Brandmeier, R.E. Dale, et al., Orientation changes of the myosin light chain domain during filament sliding in active and rigor muscle, J. Mol. Biol. 318 (2002) 1275–1291.
[27] R.E. Dale, S.C. Hopkins, U.A. an der Heide, T. Marszalek, M. Irving, Y.E. Goldman, Model-independent analysis of the orientation of fluorescent probes with restricted mobility in muscle fibers, Biophys. J. 76 (1999) 1606–1618.
[28] B. Brenner, E. Eisenberg, Rate of force generation in muscle: correlation with actomyosin ATPase activity in solution, Proc. Natl. Acad. Sci. U. S. A. 83 (1986) 3542–3546.
[29] T. Kampourakis, X. Zhang, Y.B. Sun, M. Irving, Omecamtiv Mercabil and Blebbistatin modulate cardiac contractility by perturbing the regulatory state of the myosin filament, J. Physiol. 596 (2018) 31–46.
[30] T. Kampourakis, M. Irving, Phosphorylation of myosin regulatory light chain controls myosin head conformation in cardiac muscle, J. Mol. Cell. Cardiol. 85 (2015) 199–206.
[31] K. Kazmierczak, P. Muthu, W. Huang, M. Jones, Y. Wang, D. Szczesna-Cordary, Myosin regulatory light chain mutation found in hypertrophic cardiomyopathy patients increases isometric force production in transgenic mice, Biochem. J. 442 (2012) 95–103.
[32] J. Ratti, E. Rostkova, M. Gautel, M. Pfuhl, Structure and interactions of myosin-binding protein C domain C0: cardiac-specific regulation of myosin at its neck? J. Biol. Chem. 286 (2011) 12650–12658.
[33] Y. Ait-Mou, K. Hsu, G.P. Farman, M. Kumar, M.L. Greaser, T.C. Irving, et al., Titin strain contributes to the Frank-Starling law of the heart by structural rearrangements of both thin- and thick-filament proteins, Proc. Natl. Acad. Sci. U. S. A. 113 (2016) 2306–2311.
[34] X. Zhang, T. Kampourakis, Z. Yan, I. Sevrieva, M. Irving, Y.B. Sun, Distinct contributions of the thin and thick filaments to length-dependent activation in heart muscle, elife 6 (2017) e24081.
[35] V. Sequeira, P.J. Wijnker, L.L. Nijenkamp, D.W. Kuster, A. Najafi, E.R. Witjas-Paalberends, et al., Perturbed length-dependent activation in human hypertrophic cardiomyopathy with missense sarcomeric gene mutations, Circ. Res. 112 (2013) 1491–1505.
[36] M. Gruen, M. Gautel, Mutations in beta-myosin S2 that cause familial hypertrophic cardiomyopathy (FHC) abolish the interaction with the regulatory domain of myosin-binding protein-C, J. Mol. Biol. 286 (1999) 933–949.
[37] H.S. Jung, S. Komatsu, M. Ikebe, R. Craig, Head-head and head-tail interaction: a general mechanism for switching off myosin II activity in cells, Mol. Biol. Cell 19 (2008) 3234–3242.
[38] M. Linari, E. Brunello, M. Reconditi, L. Fusi, M. Caremani, T. Narayanan, et al., Force generation by skeletal muscle is controlled by mechanosensing in myosin filaments, Nature 528 (2015) 276–279.
[39] Y. Wang, K. Ajtai, T.P. Burghardt, Ventricular myosin modifies in vitro step-size when phosphorylated, J. Mol. Cell. Cardiol. 72 (2014) 231–237.
[40] M. Kumar, S. Govindan, M. Zhang, R.J. Khairallah, J.L. Martin, S. Sadayappan, et al., Cardiac myosin-binding protein C and troponin-I phosphorylation independently modulate myofilament length-dependent activation, J. Biol. Chem. 290 (2015) 29241–29249.
[41] J.A. Spudich, Hypertrophic and dilated cardiomyopathy: four decades of basic research on muscle lead to potential therapeutic approaches to these devastating

genetic diseases, Biophys. J. 106 (2014) 1236–1249.
[42] A.J. Marian, Pathogenesis of diverse clinical and pathological phenotypes in hypertrophic cardiomyopathy, Lancet 355 (2000) 58–60.
[43] J.G. Crilley, E.A. Boehm, E. Blair, B. Rajagopalan, A.M. Blamire, P. Styles, et al., Hypertrophic cardiomyopathy due to sarcomeric gene mutations is characterized by impaired energy metabolism irrespective of the degree of hypertrophy, J. Am. Coll. Cardiol. 41 (2003) 1776–1782.
[44] G. Cuda, L. Fananapazir, W.S. Zhu, J.R. Sellers, N.D. Epstein, Skeletal muscle expression and abnormal function of beta-myosin in hypertrophic cardiomyopathy, J. Clin. Invest. 91 (1993) 2861–2865.
[45] F.I. Malik, J.J. Hartman, K.A. Elias, B.P. Morgan, H. Rodriguez, K. Brejc, et al., Cardiac myosin activation: a potential therapeutic approach for systolic heart failure, Science 331 (2011) 1439–1443.
[46] E.M. Green, H. Wakimoto, R.L. Anderson, M.J. Evanchik, J.M. Gorham, B.C. Harrison, et al., A small-molecule inhibitor of sarcomere contractility suppresses hypertrophic cardiomyopathy in mice, Science 351 (2016) 617–621.
[47] J. Huang, J.M. Shelton, J.A. Richardson, K.E. Kamm, J.T. Stull, Myosin regulatory light chain phosphorylation attenuates cardiac hypertrophy, J. Biol. Chem. 283 (2008) 19748–19756.
[48] P. Ding, J. Huang, P.K. Battiprolu, J.A. Hill, K.E. Kamm, J.T. Stull, Cardiac myosin light chain kinase is necessary for myosin regulatory light chain phosphorylation and cardiac performance in vivo, J. Biol. Chem. 285 (2010) 40819–40829.
[49] C.C. Yuan, P. Muthu, K. Kazmierczak, J. Liang, W. Huang, T.C. Irving, et al., Constitutive phosphorylation of cardiac myosin regulatory light chain prevents development of hypertrophic cardiomyopathy in mice, Proc. Natl. Acad. Sci. U. S. A. 112 (2015) E4138–46.